# A Design of Phase-Shifted FB-ZVS PWM Converter for Driving Magnetron and Its Average Anode Current Controller

Wan-Yun Lee, Gyo-Bum Chung, Pan-Seok Shin

Department of Electrical Engineering
Hongik University, Jochiwon, Chungnam, KOREA, 339-701
Tel: +82-41-860-2595, Fax: +82-41-863-7605
wylee@won.hongik.ac.kr, gbchung@wow.hongik.ac.kr, psshin@wow.hongik.ac.kr

***Abstract*** **— This paper proposes to use a 20[kHz] phase-shifted Full-Bridge (FB) Zero-Voltage-Switched (ZVS) PWM converter in order to drive a 600[W] magnetron, and analyzes the operational modes in a switching period. Additionally, the controller of the average anode current is designed. Simulation studies and experiments verify that the proposed converter and the average anode current controller shows good performance to drive the magnetron.**

***Keyword*** **– Magnetron, ZVS, Phase-shifted FB-ZVS PWM Converter, HFHVT**

## I. INTRODUCTION

A conventional driving circuit of microwave oven in Fig. 1 has thyristors, a 60[Hz] high voltage transformer (HVT) of heavy weight, a high voltage capacitor of large size in the voltage doubler circuit in order to control the magnitude of the magnetron anode-to-cathode voltage. The microwave oven has two disadvantages of heavy weight and low efficiency. Also, it has not a controller for the constant anode current of the magnetron. However, industrial microwave generators are asked to control the anode current of the magnetron for the constant output power.

Therefore, this paper proposes to use a phase-shifted full-bridge zero-voltage-switched PWM converter for driving a 600[W] magnetron, in which IGBTs instead of thyristors are used, the switching frequency is increased from 60[Hz] to 20[kHz] and the average anode current controller is adopted.

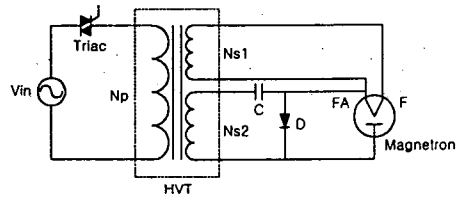


Fig. 1 A conventional driving circuit for magnetron

## II. MAGNETRON

### A. Characteristics of Magnetron

In general, magnetrons with the cut-off voltage of 3.7~3.8[kV] at 60[Hz] generate the microwave of 2450[MHz] when the supply voltage is above the cut-off voltage. Filament of magnetron needs about 3.3[V] in order to emit electrons from the cathode. The anode current, flowing to the cathode of the magnetron, is 0.3[A].

### B. Equivalent circuit of Magnetron

Fig. 2 shows an equivalent circuit of a magnetron, which consists of a diode D for the current direction and a zener diode $D_Z$ for the magnetron cut-off voltage.

In the equivalent circuit, the magnetron is considered as a resistor $R_O$ when the supply voltage is below the cut-off voltage, and a resistor $R_I$ above the cut-off voltage.[1][2]

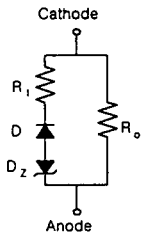


Fig. 2 The equivalent circuit of magnetron

## III. PHASE-SHIFTED FB-ZVS PWM CONVERTER FOR DRIVING MAGNETRON

### A. Configuration of circuit

Fig. 3 shows the main circuit of the phase-shifted FB-ZVS PWM converter for driving a magnetron, which has four IGBTs, High Frequency Transformer (HFT:$T_1$) to heat the filament, High Frequency High Voltage Transformer (HFHVT:$T_2$)[3][4], high voltage capacitor $C_1$ and high voltage diode $D_1$ and $D_2$ to generate the high voltage for the magnetron.

### B. Operational principles

The characteristics of magnetron can be described with a piecewise-linear model as shown in Fig. 2, which is non-linear. Therefore, it is not easy to analyze the operational characteristics of the proposed converter system with a magnetron load, comparing with a conventional DC/DC phase-shifted FB-ZVS PWM converter.[5]

Fig. 4 shows the gating signals, voltages and currents in the converter system. In Fig. 4, a switching period is subdivided into 12 sections. Fig. 5 shows the equivalent circuits corresponding to 12 sections.

**Mode 0** ($t_0 \le t < t_1$): The current I at the primary side of the HFHVT($T_2$) freewheels through diode $D_{p1}$, switch $Q_4$ and the magnetizing inductor of HFHVT($T_2$). Switch $Q_1$ can be turned on with the zero voltage switching condition.

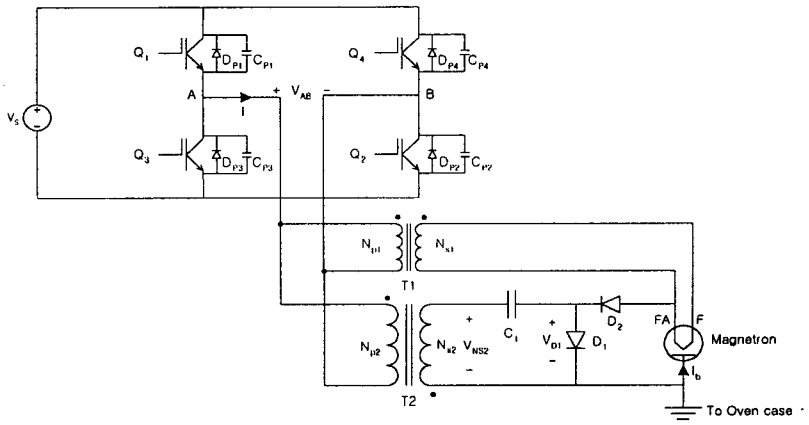


Fig. 3 Main power circuit of proposed converter for driving magnetron

The magnitude of voltage across the high voltage diode $D_1$ is equal to $V_{C1}$[V] and the magnitude of the secondary voltage of the transformer HFHVT($T_2$), $V_{NS2}$, is 0[V].

**Mode 1** ($t_1 \le t < t_2$) : It is a dead time section after switch $Q_4$ turns off. The stray capacitor, $C_{P4}$, is charged to $V_S$[V] and $C_{P2}$ is discharged to 0[V]. The current, I, flows through the magnetizing inductor of the primary side of HFHVT($T_2$) and diode $D_{P1}$.

**Mode 2** ($t_2 \le t < t_3$) : Due to the voltage at the secondary of HFHVT($T_2$) and the capacitor voltage $V_{C1}$, magnetron starts oscillating and diode $D_2$ in the voltage doubler circuit turns on.

**Mode 3** ($t_3 \le t < t_4$) : Diode $D_{p2}$ turns on. The current I at the primary side of HFHVT($T_2$) returns the energy of the magnetizing inductor to source. However, the magnetron oscillates due to the cut-off voltage generated by the voltage doubler. The magnetron is energized from the magnetizing inductor and the doubler capacitor.

**Mode 4** ($t_4 \le t < t_5$) : The current, I, at the primary side current of HFHVT($T_2$) changes its direction from B-A to A-B and the magnetron continues to oscillate. The magnetron is energized from the voltage source, $V_s$.

**Mode 5** ($t_5 \le t < t_6$) : It is a dead time section after switch $Q_1$ turns off. $C_{P1}$ starts being charged to $V_S$[V], $C_{P3}$ discharged to 0[V]. Due to the energy stored in magnetizing and leakage inductors at the primary side of HFHVT($T_2$), the current I flows through the magnetizing inductor and switch $Q_2$.

**Mode 6** ($t_6 \le t < t_7$) : After $C_{P3}$ is discharged to 0[V], the diode $D_{P3}$ turns on. Switch $Q_3$ can be turned on with the zero voltage switching condition. However, the direction of the current, I, is not changed.

**Mode 7** ($t_7 \le t < t_8$) : It is a dead time section. When $Q_2$ turns off, $C_{P2}$ is charged to $V_S$[V] and $C_{P4}$ is discharged to 0[V]. The primary side current of HFHVT($T_2$) freewheels through diode $D_{p3}$ and transfers energy to source $V_s$.

**Mode 8** ($t_8 \le t < t_9$) : The direction of the primary side current of HFHVT($T_2$) is equal to the one in the mode 7. The voltage doubler capacitor $C_1$ starts charging to $V_{NS2}$[V], which is the magnitude of the secondary side voltage of HFHVT($T_2$). In this mode, Switch $Q_4$ can be turned on with the zero voltage switching condition.

**Mode 9** ($t_9 \le t < t_{10}$) : The primary side current, I, of HFHVT($T_2$) changes its direction from A-B to B-A through switches $Q_3$ and $Q_4$. $C_1$ continues to be charged to $V_{NS2}$[V]. The length of the mode depends on the capacitance of $C_1$.

**Mode 10** ($t_{10} \le t < t_{11}$) : After finishing the charging process of the doubler capacitor $C_1$, the voltage source $V_S$ energizes the magnetizing inductor. $D_1$ continues to conduct because of ESR and the diode forward voltage drop.

**Mode 11** ($t_{11} \le t < t_{12}$) : Mode 11 is a dead time section. The stray capacitor $C_{P1}$ is discharged to 0[V] and $C_{P3}$ is charged to $V_s$[V]. After finishing Mode 11, the converter goes back to mode 0 repeatedly.

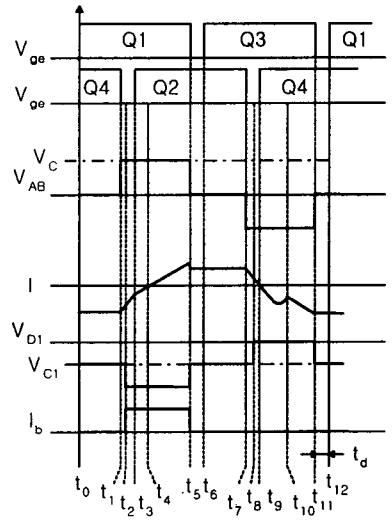


Fig. 4 Waveforms of $V_{ge}$, $V_{AB}$, I, $V_{D1}$, $I_b$

**Mode 0** ($t_0 \le t < t_1$)

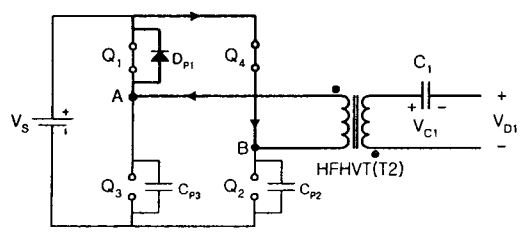


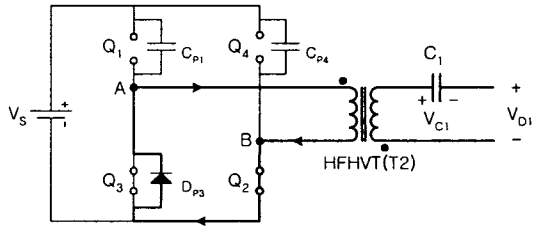


**Mode 1** $(t_1 \le t < t_2)$

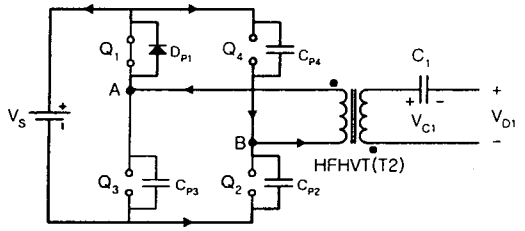


**Mode 7** $(t_7 \le t < t_8)$

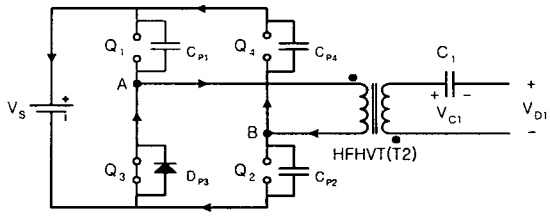


**Mode 2** $(t_2 \le t < t_3)$

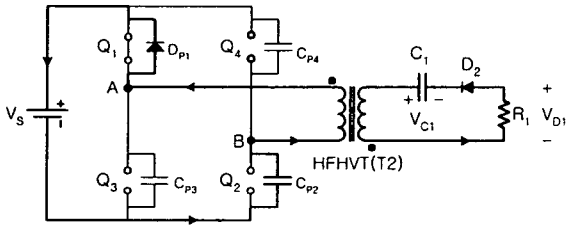


**Mode 8** $(t_8 \le t < t_9)$

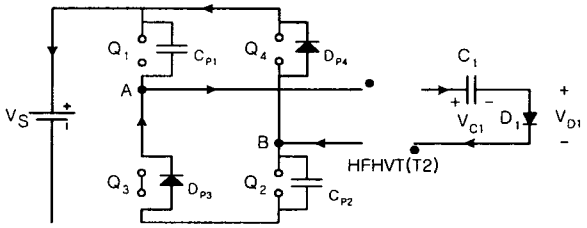


**Mode 3** $(t_3 \le t < t_4)$

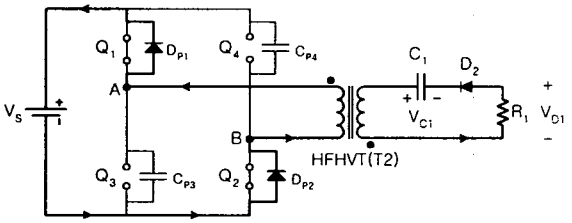


**Mode 9** $(t_9 \le t < t_{10})$

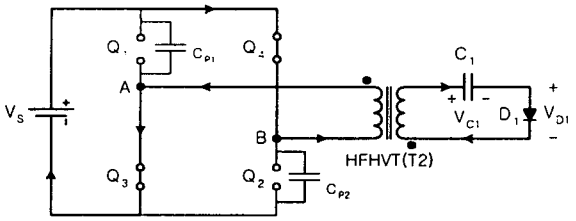


**Mode 4** $(t_4 \le t < t_5)$

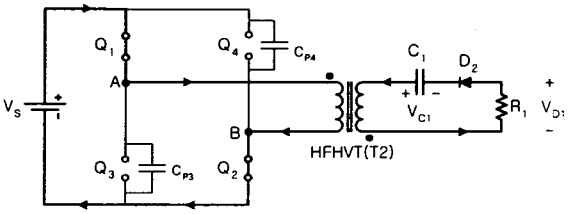


**Mode 10** $(t_{10} \le t < t_{11})$

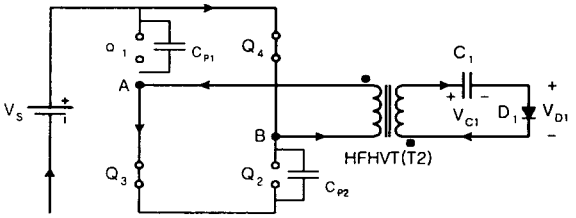


**Mode 5** $(t_5 \le t < t_6)$

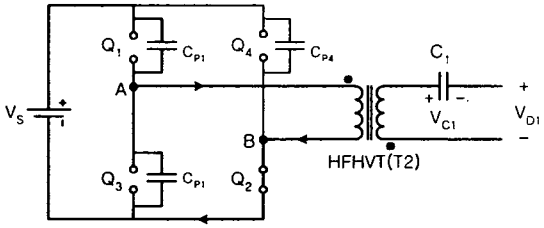


**Mode 11** $(t_{11} \le t < t_{12})$

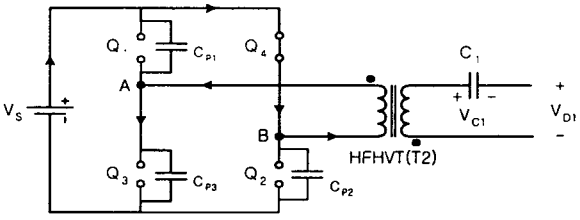


Fig. 5 Operation modes of the proposed converter in a switching period

**Mode 6** $(t_6 \le t < t_7)$

*C. Conditions for the zero voltage switching*

The phase-shifted FB-ZVS PWM converter provides zero voltage switching for all power switches in the circuit. However, the mechanism providing the zero voltage switching in each leg of the converter is different from the one in the other leg. The zero voltage switching of the proposed converter happens in mode 1, 2, 5, 7 and 11 in Fig. 5. In mode 2, the magnitude of the primary current, I, is greater than those in mode 1, 5, 7 and 11. Therefore, only mode 1 is considered for deriving the condition of zero voltage switching. Since the parameters of HFT($T_1$) is smaller than HFHVT($T_2$), HFT($T_1$) is also neglected for deriving the condition. In order to guarantee the zero voltage switching under the above assumption, the following inequality should be satisfied:

$$E = \frac{1}{2}(L_{lk} + L_m)I(t_1) \geq \frac{1}{2}C_{TR}V_{AB}^2 + \frac{4}{3}C_P V_{AB}^2 \qquad (1)$$

where $L_{lk}$ is the leakage inductance at the primary side of HFHVT(T2), $L_m$ is the magnetizing inductance of HFHVT(T2) at the primary side, I is the current of HFHVT(T2) primary side at mode 2, $V_{AB}$ is the voltage of HFHVT(T2) primary side, $C_{TR}$ is the stray capacitance of HFHVT (T2), $C_P$ is the stray capacitance of the power switches.

The proposed converter needs the dead time to protect the power switches from the short circuit. The dead time is written in eq (2).

$$t_d = \frac{T}{4} = \frac{\pi}{2}\sqrt{(L_{lk} + L_m)(C_P + C_{TR})}\ [s] \qquad (2)$$

Parameters of the proposed converter in Fig. 1 are presented in Table 1.

Table 1. Parameters of the proposed converter

| Parameter | Value | Unit |
|---|---|---|
| $V_{AB}$ | 150 | [ V ] |
| a($N_1/N_2$) | 1/15 | [ Turn ] |
| $C_1$ | 5 | [ nF ] |
| $L_{lk}$ | 7.51 | [ uH ] |
| $L_m$ | 895.49 | [ uH ] |
| $C_p$ | 1.1 | [ nF ] |
| $C_{TR}$ | 1 | [ pF ] |
| $f_r$ | 20 | [ kHz ] |

## IV. Design of Average Anode Current Controller for Phase-Shifted FB-ZVS PWM Converter for Magnetron Driving

*A. Transfer function of the proposed converter system*

In order to design the average current controller, the transfer function is derived with simplified model. Fig. 6 shows the equivalent circuit of the proposed converter system in the oscillation sections (Mode2, 3, 4), where a is the turn ratio of HFHVT($T_2$).

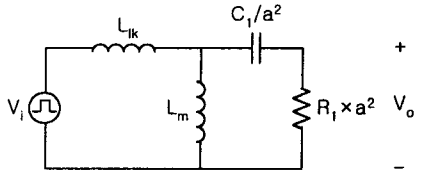


Fig. 6 An Equivalent circuit of the proposed converter

The transfer function between $V_i$ and $V_o$ is shown in Eq. (3). $V_i$ is the rectangular pulse synthesized by the power switches and $V_o$ is the anode-to-cathode voltage of the magnetron.

$$G(s) = \frac{v_o(s)}{v_i(s)} = \frac{s^2(C_1 \times L_m \times R_1)}{s^3(L_{lk} \times L_m \times C_1) + s^2(L_{lk} \times C_1 \times R_1) + s(L_{lk} + L_m + R_1)} \qquad (3)$$

Fig. 7 shows the frequency response of G(s), which means the output voltage to be directly proportional to the input voltage around the switching frequency.

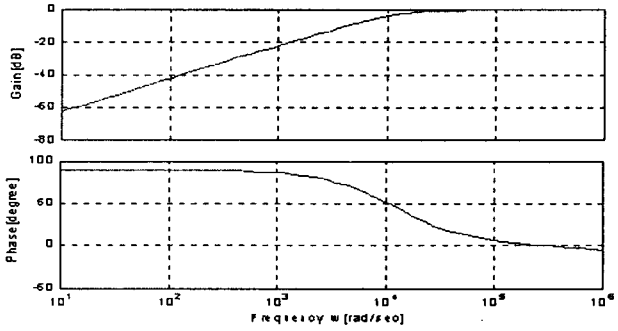


Fig. 7 Frequency response of the transfer function, G(s)

*B. Average anode current controller*

The waveform of the anode current of the magnetron, $I_b$, in Fig. 3 takes the shape of rectangular pulse. The output power of the magnetron is proportional to the average value of the anode current, $I_b$. Therefore, in order to control the output power of the magnetron, it is necessary to control the average value of the anode current. The equivalent model of magnetron in Fig. 2 and the frequency response in Fig. 7 mean that the average current is negatively proportional to the phase shift angle. Fig. 8 shows the block diagram to control the average anode current.

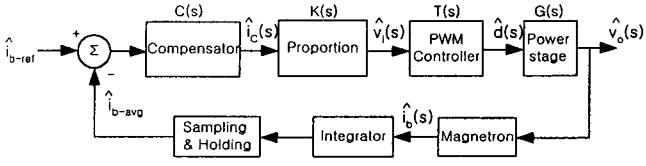


Fig. 8 Block diagram to control the average anode current

The crossover frequency of the designed average anode

current controller is assigned to 4[kHz], which is about one-fifth of the switching frequency, 20[kHz]. And the phase angle of the compensator is assigned to -90[° ] at the crossover frequency. The transfer function of the designed compensator, C(s), is shown in Eq. (4).

$$C(s) = \frac{K}{s+2} \tag{4}$$

where K is 22000. Fig. 9 shows the frequency response of the compensator.

Fig. 10 shows the loop gain of the closed-loop of proposed converter with average anode current controller, which has the slope of –20[dB/dec] at crossover frequency and the phase margin is 124[° ].

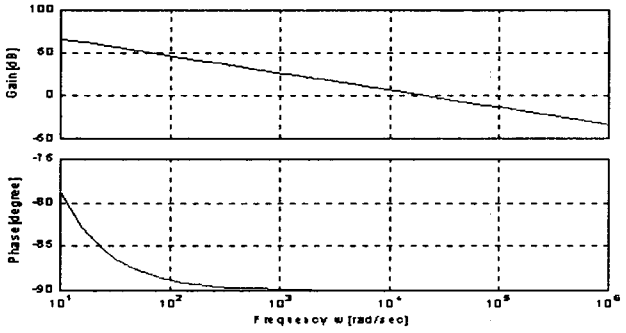


Fig. 9 Frequency response of the compensator, C(s)

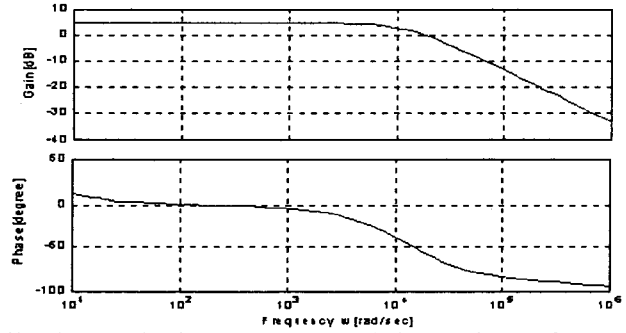


Fig. 10 Loop gain of Closed-loop proposed PS FB-ZVS PWM Converter

## V. Results of Experiment and Computer Simulation

Fig. 11 shows a waveform of $V_{AB}$ and I of the primary side of HFHVT($T_2$) without average anode current controller.

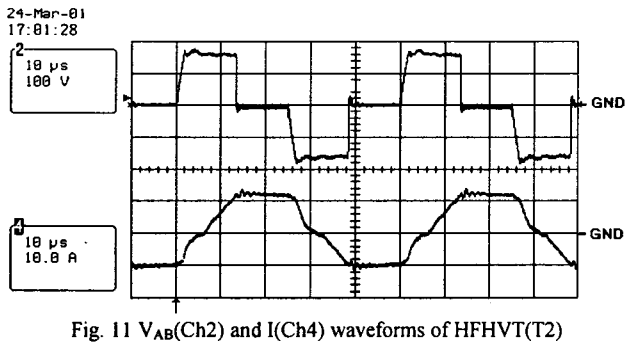


Fig. 11 $V_{AB}$(Ch2) and I(Ch4) waveforms of HFHVT(T2)

Fig. 12 shows waveforms of $V_{ge1}$, $V_{ce1}$ and $I_{c1}$, in which the zero voltage switching condition of power switch $Q_1$ is shown. Fig. 13 shows detailed waveforms of $V_{ge1}$ and $V_{ce1}$.

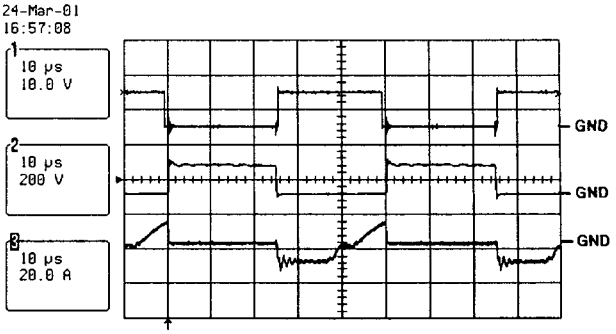


Fig. 12 Waveforms of $V_{ge1}$(Ch1), $V_{ce1}$(Ch2) and $I_{c1}$(Ch3)

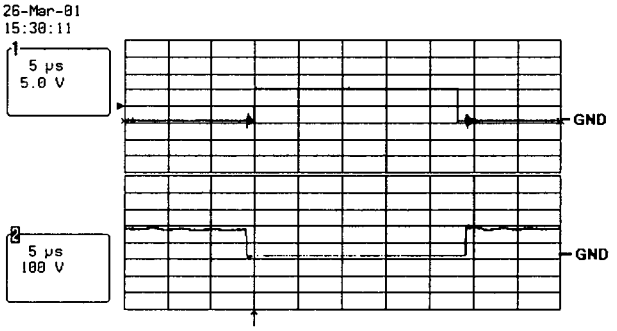


Fig. 13 Waveforms of $V_{ge1}$(Ch1) and $V_{ce1}$(Ch2)

Fig. 14, 15 show $V_{AB}$, the voltage of HFHVT($T_2$) primary side, $I_b$ , the anode current of magnetron, and $V_{D1}$ , the voltage across high voltage diode $D_1$. The waveform of $V_{D1}$ in Fig. 15 has the ringing phenomenon at 2000[V]. However, the riging does not have any effects on the osillcation of the magnetron.

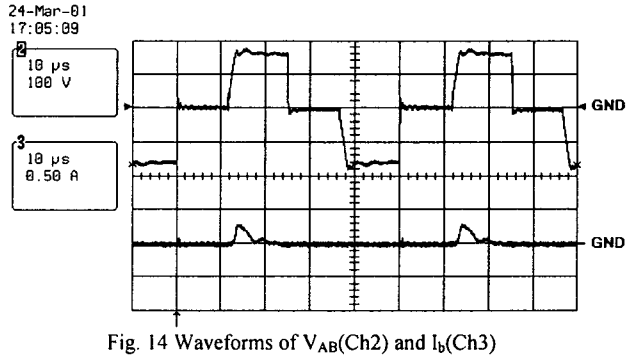


Fig. 14 Waveforms of $V_{AB}$(Ch2) and $I_b$(Ch3)

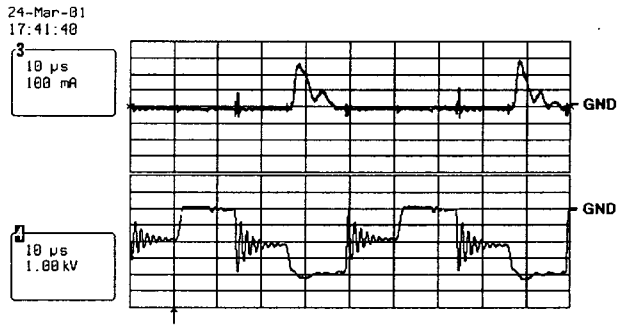


Fig. 15 Waveforms of $I_b$(Ch3) and $V_{D1}$(Ch4)

The computer simulation studies to demonstrate the characteristics of the average anode current controller are

performed. Fig. 16 shows measured-average anode current $I_{b\text{-}avg}$, reference anode current $I_{b\text{-}ref}$, and error between $I_{b\text{-}avg}$ and $I_{b\text{-}ref}$ . The reference value of average anode current is changed from 5.0[mA] to 3.0[mA] at 2.5[ms] and reversely at 7.5[ms].

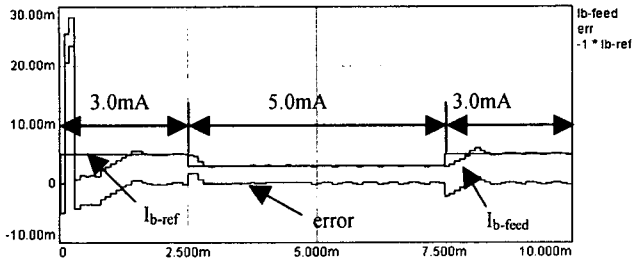


Fig. 16 Waveforms of $I_{b\text{-}avg}$, $I_{b\text{-}ref}$, and error

Fig. 17 shows the waveforms of $V_{AB}$, I, $V_{D1}$ and $I_b$, at the reference of the anode current, 5[mA]. Fig. 18 shows the waveforms of $V_{AB}$, I, $V_{D1}$, and $I_b$ at the reference of the anode current, 3.0[mA]. Fig. 19 shows the waveform of the anode current for the whole simulation period.

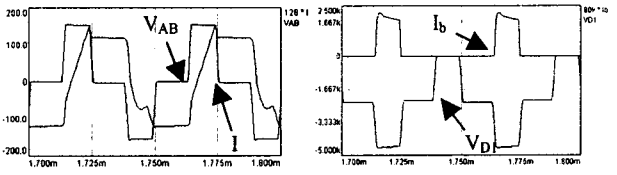


(a) $V_{AB}$, I (b) $V_{D1}$, $I_b$

Fig. 17 Waveforms of $V_{AB}$, I, $V_{D1}$, and $I_b$ at $I_{b\text{-}avg}$=5[mA]

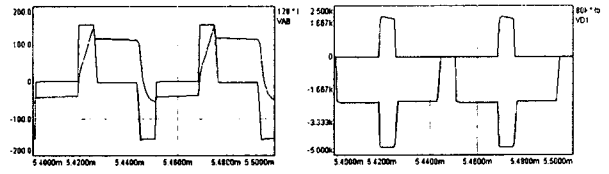

(a) $V_{AB}$, I (b) $V_{D1}$, $I_b$

Fig. 18 Waveforms of $V_{AB}$, I, $V_{D1}$ and $I_b$ at $I_{b\text{-}avg}$=3[mA]

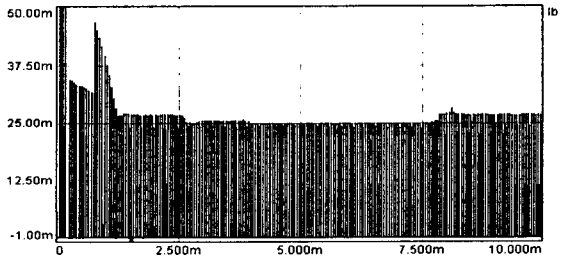


Fig. 19 Waveform of anode current $I_b$

Fig. 20 and 21 show the output waveforms of the sampler/holder, which converts the anode current of the pulse form to the average value of the anode current. The period of the sampler is $2T_{switching}$.

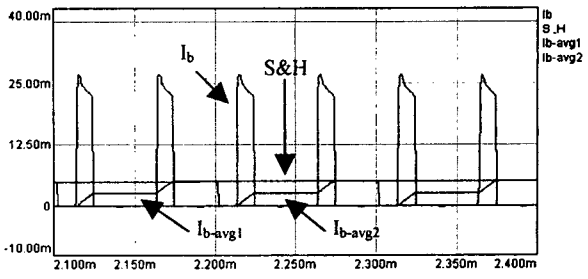


Fig. 20 Waveforms of anode current $I_b$, $I_{b\text{-}avg}$

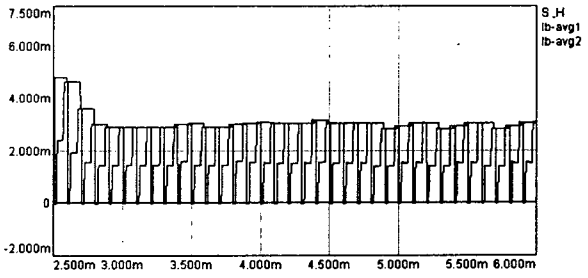


Fig. 21 Waveforms of $I_{b\text{-}avg}$, output of sampler and holder

## VI. CONCLUSIONS

This paper proposes to use a phase-shifted FB-ZVS PWM converter for driving magnetron, designs an average anode current controller for controlling the output power of the magnetron and analyzes 12 modes related to the converter operation.

As compared with the conventional 60[Hz] power converter system for driving magnetron, the proposed converter has advantages of light weight and high power density. An integrator, a sampler and a holder are added to the feedback loop of the proposed converter system, which shows to control the average anode current of the magnetron efficiently in the simulation study.

## VII. REFERENCE


1. Duk-Jin Oh, Hee-Jun Kim, "Development of Power Supply for driving high Power Magnetron in a Mircowave Oven", *Trans. of KIPE*, Vol.5 No 3, pp300~306, 2000.6
2. Wan-Yun Lee, Gyo-Bum Chung, Pan-Seok Shin, "A Design of Driving Circuit for Microwave oven using Phase-shifted FB-ZVS PWM Converter", *Trans.of KIPE*, Vol.6 No.3, pp.265~272, 2001.6
3. George Chryssis, "High-Frequency Switching Power Supplies : Theory and Design", *Mcgraw-hill*, pp.89~96, 1994
4. Colonel Wm.T.McLyman, "Magnetic Core Selection for Transform -ers and Inductor", *Marcel Dekker*, pp.104~110, 1997
5. J. Sabate, et., al., "Design Considerations for High Voltage, High Power, Full Bridge, Zero-Voltage-Switched PWM Converter", *IEEE APEC 90 Proc.*, pp.275~284, 1990